Formation of Titanium Carbide from Ilmenite Concentrates in a Thermal Plasma Reactor

PATRICK R. TAYLOR, MILTON MANRIQUE, SHAHID A. PIRZADA, AND MASUD ABDEL-LATIF

Reprinted from PLASMA CHEMISTRY AND PLASMA PROCESSING
Plenum Press

Vol. 15, No. 3, September 1995
Printed in England

Plasma Chemistry and Plasma Processing, Vol. 15, No. 3, 1995

Formation of Titanium Carbide from Ilmenite Concentrates in a Thermal Plasma Reactor

Patrick R. Taylor,[1] Milton Manrique,[2]
Shahid A. Pirzada,[1] and Masud Abdel-Latif[3]

Received August 10, 1994; revised December 5, 1994

Formation of fine titanium carbide powder, using ilmenite concentrate and methane as feed, in a thermal plasma reactor was investigated. The plasma torch was operated using argon–helium and argon–nitrogen mixtures as plasma gases. Different molar ratios of ilmenite concentrate and methane were used to study the yield of titanium carbide. The highest overall conversion of ilmenite to titanium carbide was 96%. The powders produced were subjected to physical and chemical characterization by various analytical techniques. The results of this investigation show the possibility of developing a new process to obtain valuable ceramic materials using minerals directly as raw materials.

KEY WORDS: Thermal plasma; titanium carbide; ilmenite; ceramic powder.

1. INTRODUCTION

Ilmenite ($FeTiO_3$) is the most common mineral of titanium and is used as a source of titanium. The concentration of titanium in ilmenite and related minerals varies considerably. Pure ilmenite contains 53% TiO_2, but in some sand deposits, ilmenite has been upgraded due to iron oxidation and leaching as a natural beneficiation process.

The extraction processes developed for ilmenite ores have been reviewed in recent years.[1–3] A large variety of techniques regarding ilmenite processing have been mentioned in the literature. Several processes[4–7] are related to the reaction of ores with alkali metal compounds or hydroxides where the resultant salts can then be dissolved in dilute mineral acid or water. Other processes[8–10] dissolve impurities directly using mineral acids or pre-reduced iron to the ferrous or metallic state followed by leaching of iron

[1]Department of Metallurgical and Mining Engineering, College of Mines, University of Idaho, Moscow, Idaho 83843.
[2]Department of Materials Science, Simon Bolivar University, Caracas, Venezuela.
[3]Mintek, South Africa.

and other impurities. There are some high temperature processes,[11-13], such as the smelting-carbothermic reduction to produce pig iron and high-TiO_2 slags and the selective chlorination process for the removal of certain impurities under conditions where titanium does not react with the chlorine compounds.

Recently, several new processes have been proposed for the beneficiation of ilmenite, such as the solid-state reduction with hydrogen[14,15] for the production of oxygen from lunar rocks. Ilmenite is found in abundance (up to 20%) in lunar rocks. In another study,[16] ilmenite concentrate was reduced by carbon in a temperature range 1900–2000°C, yielding titanium oxycarbide and metallic iron. Terry *et al.*[17] described a fundamental investigation of the viability of producing Fe–Ti(O, C) metal matrix composites by the one-step carbothermic reduction of pelletized mixtures of iron, rutile, or ilmenite and collie coal, using a tube furnace at 1300–1600°C under argon atmosphere. Group II halide fluxes were used to improve the reduction kinetics and promote the separation of the Ti(O, C) product from the iron phase. Brown[18] investigated the reduction of ilmenite ore in a plasma jet using hydrogen as reductant. The consolidated product obtained was mainly titanium dioxide and metallic iron, while the unconsolidated fine powder was predominantly metallic iron and ilmenite. Chase and Skrivan[18] studied the reduction of titaniferous ores (ilmenite and leucoxene) in a 50-kW DC plasma torch hot-wall reactor system, using methane as a reducing agent. The product obtained was mainly TiO_2 and metallic iron which was leached easily with hydrochloric acid to obtain a final product with TiO_2 content over 90%. Yahozhong *et al.*[19] smelted enriched ilmenite using a transferred arc plasma furnace, producing a Ti-enriched slag containing 90–98% TiO_2 and molten iron. A mixture of ilmenite and charcoal powder or pre-reduced ilmenite was used as the feed material.

The present study describes the fundamental thermodynamics and the experimental results for the formation of titanium carbide and metallic iron by the reduction of ilmenite concentrates in a nontransferred arc plasma tubular reactor, using methane as a reductant.

2. THERMODYNAMICS

Free energy minimization plots for the Ti–Fe–O–C–H–N system have been developed using the CSIRO thermopackage.[20] Plasma gases are also taken into account in these thermodynamic calculations, but are not shown in the plots due to their higher contents. Figure 1 shows the thermodynamic equilibrium diagram for the system ilmenite and methane with a molar ratio of 1:4, which is the stoichiometric ratio for the overall reaction of the

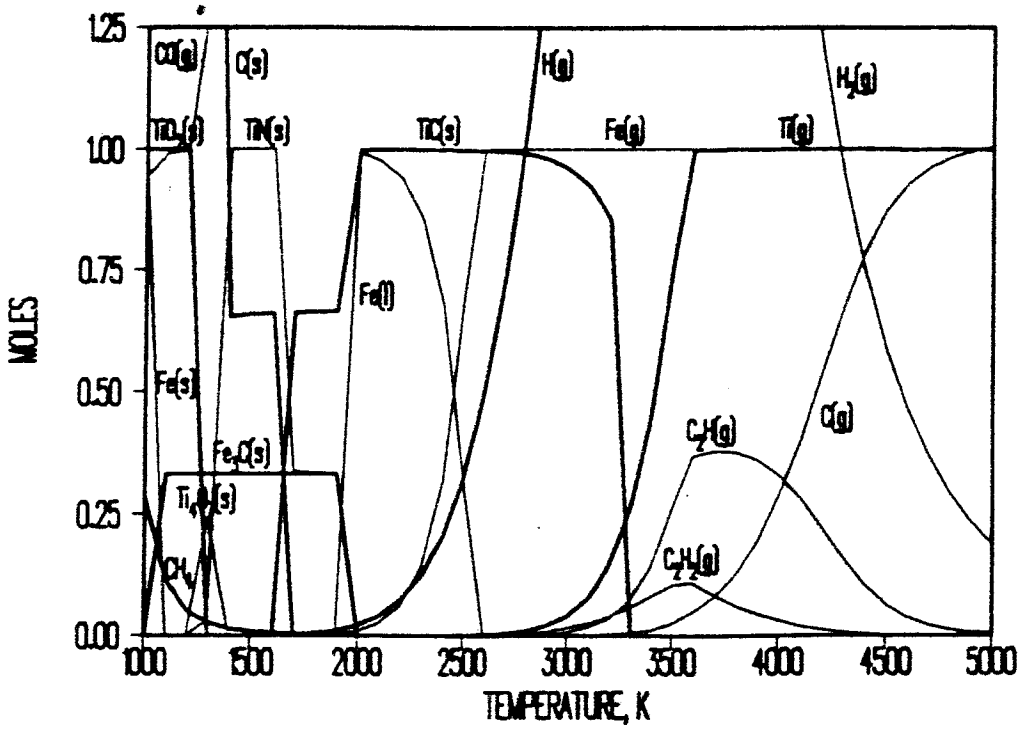

Fig. 1. Free-energy minimization plot for $FeTiO_3$:CH_4 (1:4).

titanium carbide synthesis, expressed as follows:

$$FeTiO_3(s) + 4CH_4(g) = TiC(s) + Fe(l) + 3CO(g) + 8H_2(g) \quad (1)$$

This plot shows that at temperatures above 5000 K, which are found inside the plasma jet, only the monatomic gases Ti, Fe, C, and H are stable. In the temperature range 3000–5000 K, which corresponds to the vaporization zone, some species become unstable and begin to recombine. For example, carbon combines with hydrogen to form C_2H and C_2H_2, and titanium gas combines with carbon compounds to form titanium carbide. Iron gas remains stable in this zone. Some of the possible reactions that may take place in this zone (3000–5000 K) during the reaction process are

$$2C(g) + 2H(g) = C_2H_2(g) \quad (2)$$

$$2C(g) + H(g) = C_2H(g) \quad (3)$$

$$C_2H(g) + 2Ti(g) = 2TiC(s) + H(g) \quad (4)$$

$$2Ti(g) + C_2H_2(g) = 2TiC(s) + 2H(g) \quad (5)$$

$$Ti(g) + C(g) = TiC(s) \quad (6)$$

In the temperature range 2000–3000 K which corresponds to the reaction zone in the plasma reactor, titanium carbide formed previously remains stable. At 2600 K iron gas starts condensing to form liquid iron. This calculation confirms, thermodynamically, the feasibility of producing

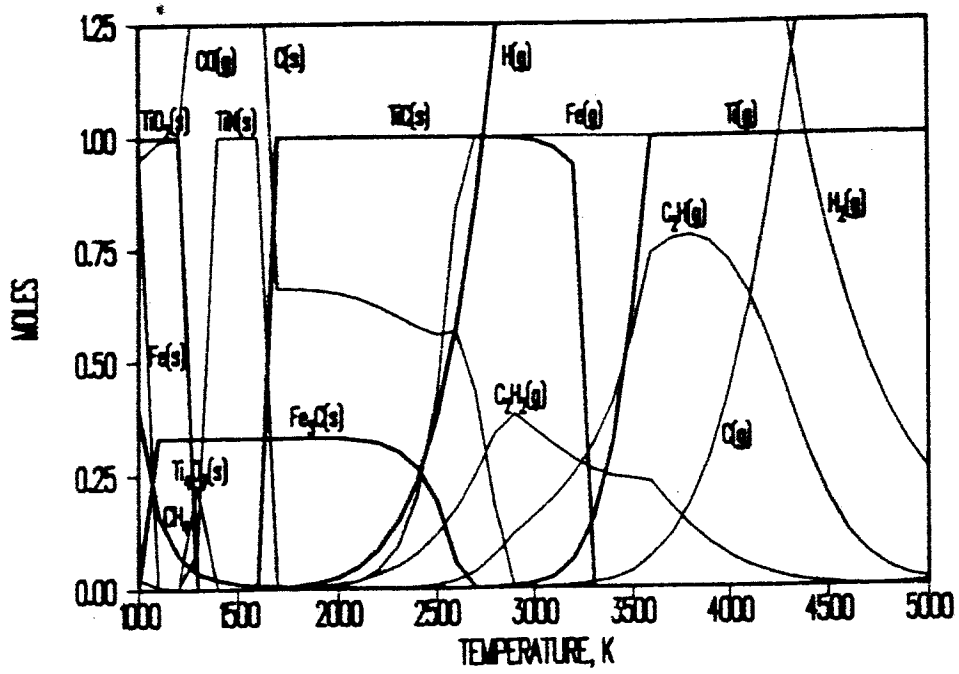

Fig. 2. Free-energy minimization plot for $FeTiO_3$:CH_4 (1:7) (plasma gas Ar–N_2).

titanium carbide and metallic iron by a quenching process. The characteristics of the product may be predicted by thermodynamics. If the quenching temperature is above 2600 K, titanium carbide particles may become nuclei for iron gas condensation, and if the quenching process starts below 2500 K, the product may be a mixture of titanium carbide particles and metallic iron particles.

At temperatures below 2000 K, which corresponds to the reoxidation (rapid quenching) zone in the plasma reactor, titanium carbide becomes unstable and recombines to form titanium oxides and/or titanium nitride, if nitrogen is present in the system. Liquid iron becomes unstable and reacts with carbon to form iron carbides. The possible reactions taking place in this zone during the cooling process are as follows:

$$2TiC(s) + N_2(g) = 2TiN(s) + 2C(s) \quad (7)$$

$$3Fe(l) + C(s) = Fe_3C(s) \quad (8)$$

$$4TiC(s) + 7CO(g) = Ti_4O_7(s) + 11C(s) \quad (9)$$

$$Ti_4O_7(s) + CO(g) = 4TiO_2(s) + C(s) \quad (10)$$

Comparing the free energies of formation for the above-mentioned reactions, reaction (9) is the most likely in this temperature range (below 2000 K) and thus may be responsible for titanium carbide oxidation.

Figure 2 shows the thermodynamic equilibrium diagram for the system $FeTiO_3$:CH_4 with a molar ratio of 1:7. The presence of excess methane

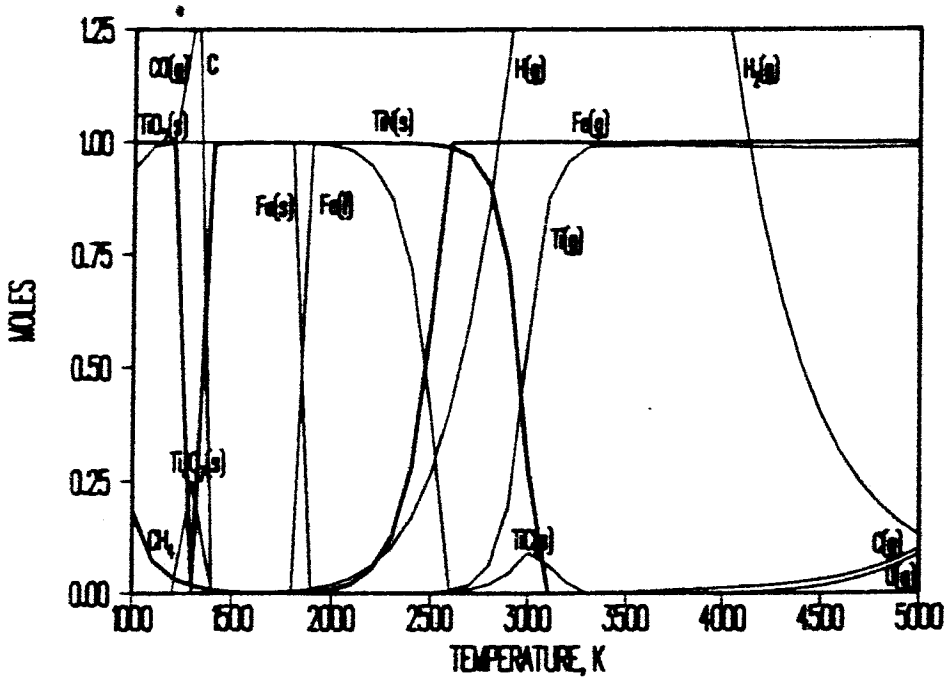

Fig. 3. Free-energy minimization plot for $FeTiO_3$:CH_4 (1:3) (plasma gas Ar–N_2).

increases the relative amounts of the species containing carbon as well as their range of stability. The main features of the system are as follows: Solid titanium carbide becomes stable in the temperature range 1600–3350 K, while liquid iron becomes unstable. Solid carbon stability overlaps part of the titanium carbide stability region. Iron carbide becomes stable in the temperature range 1000–2700 K, overlapping part of the titanium carbide stability region. The characteristics of the product may be predicted by thermodynamics. If the quenching process is carried out at temperatures above 2500 K, the product may contain titanium carbide particles coated by metallic iron, as well as carbon particles coated by metallic iron.

Figure 3 shows the thermodynamic equilibrium diagram of the system $FeTiO_3$:CH_4 with a molar ratio of 1:3. In this case titanium carbide becomes unstable as well as $C_2H(g)$ and $C_2H_2(g)$ and titanium nitride becomes stable in the temperature range 1300–3100 K. The product obtained in the quenching process may be formed as titanium nitride particles mixed with metallic iron particles.

Figure 4 shows the thermodynamic equilibrium diagram of the system $FeTiO_3$:CH_4 with a molar ratio of 1:4. Helium is used in the plasma gas mixture instead of nitrogen. The system is quite similar to that shown in Fig. 1 except that no nitrogen compounds exist and the solid iron stability region becomes wider.

According to the thermodynamic analysis, it can be concluded that the molar ratio and the quench temperature are the most important parameters

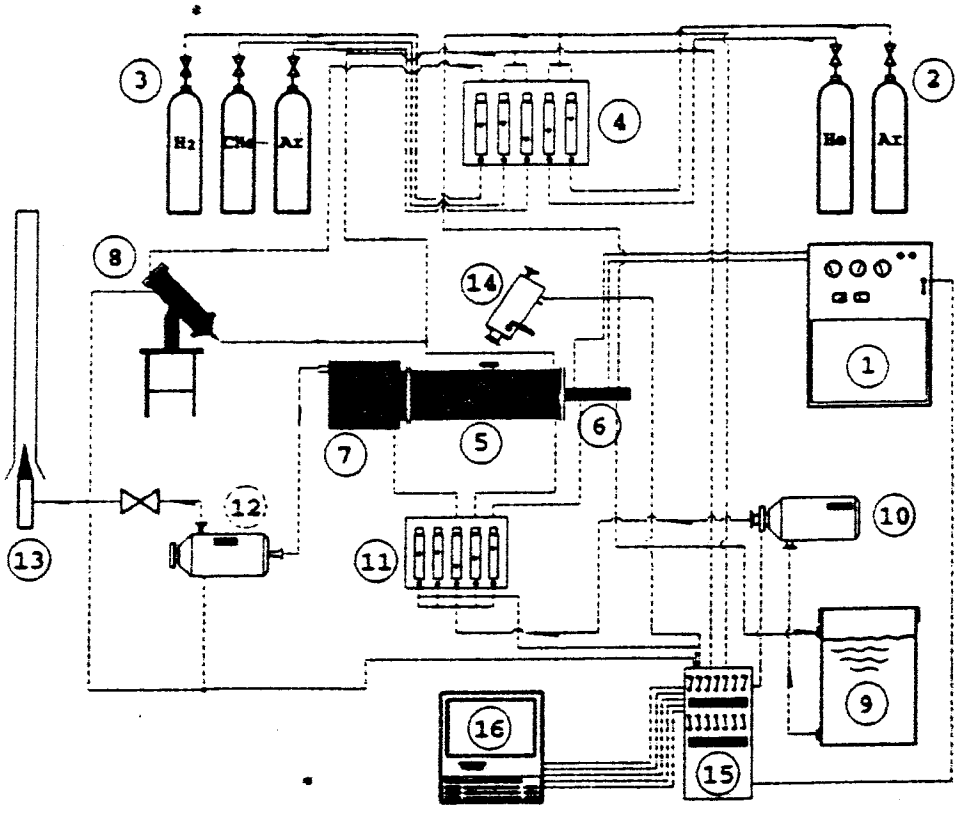

Fig. 5. Schematic of the experimental system. (1) Power supply; (2) plasma gases; (3) carrier gases; (4) gas flowmeters; (5) reactor; (6) plasma torch; (7) quench chamber; (8) powder feeder; (9) water tank; (10) water pump; (11) water flowmeters; (12) filter; (13) burner; (14) pyrometer; (15) data acquisition; (16) computer.

particles were in the size range of 10–50 μm. The chemical composition of the ilmenite concentrates used is given in Table I.

Methane is fed along with the ilmenite concentrate powder and acts as a carrier gas. It is mixed with argon gas to maintain a constant flow rate. The ilmenite feed rate was 5.0 g/min. The plasma gas flow rate used was of the order of 99–113 slpm (3.5–4.5 scfm). The general operating conditions for the plasma torch are given in Table II.

The plasma torch was started with argon, and after stabilizing, nitrogen gas was added in the required amount to reach the operating power. The reactor was preheated until it reached the required temperature. After attaining thermal equilibrium in the reactor, feeding was started. The feeding time was 25 min during which the temperatures at the different points in the reactor were continuously monitored. After the feeding stopped, the whole

Table I. Chemical Composition of Ilmenite Concentrates

Sample	TiO_2	FeO	SiO_2	MgO	MnO	Al_2O_3
1	67.37	28.30	2.98	0.16	1.02	0.55
2	47.80	42.65	3.21	0.03	1.19	0.62

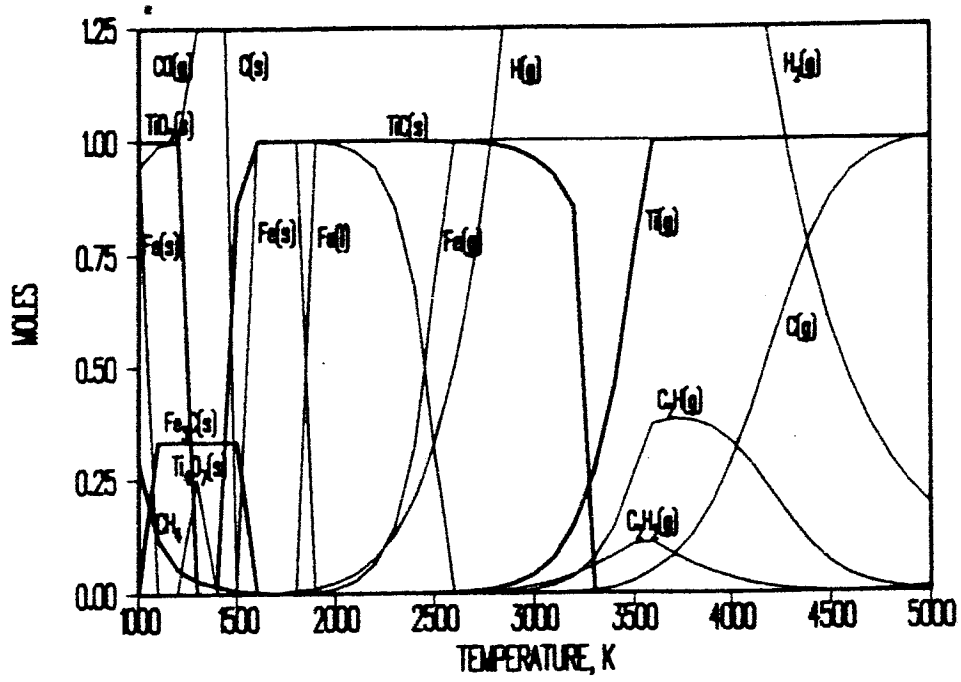

Fig. 4. Free energy minimization plot for $FeTiO_3$:CH_4 (1:4) (plasma gas Ar–He).

to be taken into consideration in order to optimize the quality of the solid product obtained.

3. EXPERIMENTAL SYSTEM

A schematic of the experimental system is shown in Fig. 5. The experimental system consists of a tubular reactor, nontransferred arc thermal plasma torch, rapid quench section, filter, powder feeder, and data acquisition system. A detailed description of this system can be found elsewhere.[21] The solid product is collected from three different points: from the inside wall of the reaction tube, the quench section, and the filter. A mixture of argon and nitrogen was used as the plasma gas. The solid and gaseous reactants are fed into the reactor, using a powder feeder, through a water-cooled injection probe inserted on an angle near the plasma jet. The gaseous stream leaving the quench section is passed through the filter and a liquid trap before venting to a stack.

4. EXPERIMENTAL PROCEDURE

Ilmenite concentrate and technical grade methane were the primary reactants. Two different types of ilmenite concentrates were used, sample No. 1 supplied by RGC Mineral Sand Inc. (USA), and sample No. 2 from the Parguaza river heavy minerals deposit in Venezuela. The size distribution of the ilmenite concentrates was measured using a sedigraph. Most of the

Table II. Typical Operating Parameters of the Plasma Torch

Parameter	Range
Voltage, V	165–185
Current, A	175–190
Power, kW	28.9–35.2
Argon flow, slpm (scfm)	99–113 (3.5–4.0)
Nitrogen flow, slpm (scfm)	14–28 (0.5–1.0)
Carrier gas, slpm (scfm)	7.0 (0.25)

Table III. Results of Experiments

Experiment number[a]	Power kW	Plasma gas	$FeTiO_3$:CH_4 Ratio	Feed, g/min	Conversion[b] of TiC, %	Recovery[c] of Fe, %
TiC-1(V)	30	Ar–N_2	1:4	4.9	96.8	60.0
TiC-2(V)	30	Ar–N_2	1:4	4.3	84.5	57.1
TiC-3(V)	31	Ar–N_2	1:7	3.1	85.0	80.8
TiC-4(A)	28	Ar–He	1:4	6.5	87.0	40.4
TiC-5(A)	30	Ar–N_2	1:4	5.8	69.4	21.0

[a](V) Venezuelan concentrate; (A) American concentrate.
[b]Conversion of ilmenite to TiC based on titanium in the feed.
[c]Iron in the product.

Table IV. Material Balance

Experiment number	Material fed, g	Product from QB, g	Product from filter, g	Product from reactor, g	Conversion of TiC, %
TiC-1(V)	97.1	15.9	19.8	23.9	96.8
TiC-2(V)	215.0	40.0	33.9	42.3	84.5
TiC-3(V)	61.3	22.2	41.5	26.5	85.0
TiC-4(A)	113.7	15.4	14.8	32.1	87.0
TiC-5(A)	161.8	18.6	14.3	31.9	69.4

system was shut down and allowed to cool under an argon atmosphere. The product was removed from the quenching box, from the filter, and from the inner wall of the reaction tube.

5. RESULTS

The results of a series of experiments are shown in Table III. The power used was kept almost constant, while the $FeTiO_3$:CH_4 molar ratio, type of plasma gas mixture, and feeding rate were varied. A complete material balance for each experiment, showing the weights of the material collected from the different sections of the reactor and overall recovery, is presented in Table IV.

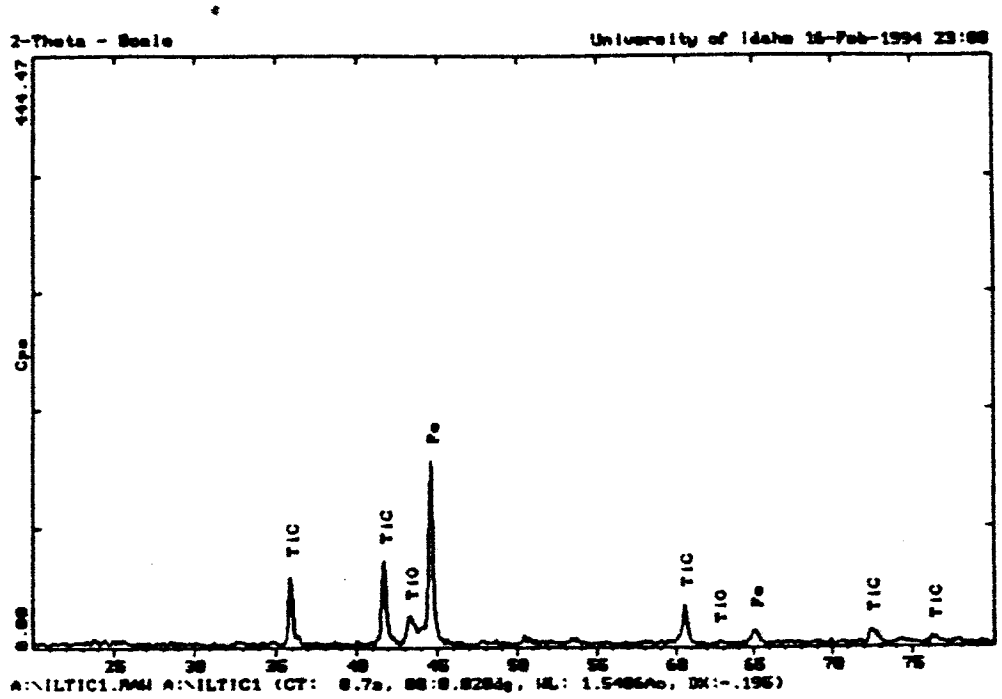

Fig. 6. X-ray diffraction patterns of the solid product collected from the quench chamber.

The solid products obtained in each run were characterized physically and chemically. Figure 6 shows a typical X-ray diffraction pattern of the solid product obtained in the cooling chamber for one of the tests performed feeding the stoichiometric molar ratio (1:4). The major components in the product are titanium carbide (TiC) and metallic iron (Fe) with minor amounts of TiO. Graphite and iron carbide are also found as major components in the solid product obtained in tests performed with an excess of methane ($FeTiO_3$:CH_4 with a molar ratio of 1:7).

A fraction of the solid products obtained in each test was dissolved in HF–HNO_3 solution at 338 K for 6 h, and the filtrate was analyzed by atomic absorption spectrometry. The solid residue left after dissolution was identified as a mixture of graphite and silicon carbide. The results of the chemical analysis are given in Table V.

Titanium–iron segregation is one of the common characteristics of these results, as can be seen by observing the Ti/Fe ratio for the different products. As a result of this phenomena, titanium carbide tends to remain in the reactor while iron is preferentially found in the quenching box and filter products due to the higher volatility of iron. Experiment TiC-3, with an excess methane, indicates the highest titanium carbide recovery, but the product has an excessive amount of carbon. Products obtained from TiC-4, using argon–helium plasma gas mixtures, present the lowest values of iron content and relatively low graphite content.

Leaching tests were carried out to remove iron from the different products of the reactor. Iron from the products obtained using argon–nitrogen

Table V. Chemical Analysis of the Solid Products, wt.%

Experiment number	Product	Ti(%)	Fe(%)	Si(%)	Mn(%)	C(%)	Ti/Fe
TiC-1	F[a]	29.5	47.1	2.9	2.4	8.9	0.63
	Q.B.[b]	31.9	46.9	2.6	2.2	6.9	0.68
	R[c]	66.5	11.0	1.7	0.1	2.6	6.06
TiC-2	F	37.2	48.3	2.7	2.8	3.4	0.77
	Q.B.	33.5	48.3	2.5	2.3	3.0	0.69
	R	61.3	12.2	2.2	0.1	7.9	5.02
TiC-3	F	12.5	19.0	1.4	0.8	62.4	0.66
	Q.B.	11.3	18.0	1.2	0.7	65.3	0.63
	R	27.1	17.3	1.5	0.1	46.6	1.57
TiC-4	F	35.7	34.2	1.3	3.1	15.5	1.04
	Q.B.	37.5	33.0	1.2	2.8	15.0	1.14
	R	53.3	16.0	1.2	0.2	15.4	3.33
TiC-5	F	38.5	24.5	1.0	3.1	22.2	1.57
	Q.B.	36.5	26.2	1.0	3.0	23.1	1.39
	R	62.0	9.4	1.0	0.2	11.4	6.60

[a]Filter; [b]quenching box; [c]reactor.

mixture as plasma gas cannot be removed completely by leaching with hydrochloric acid. Ferric chloride solution (20%) dissolved iron much better from these products, leaving some iron still undissolved. Iron was removed completely with hydrochloric acid from the products obtained using argon–helium mixture as plasma gas. All the leaching tests were carried out at 338 K for 6 h. Figure 7 shows an X-ray diffraction pattern for the quench

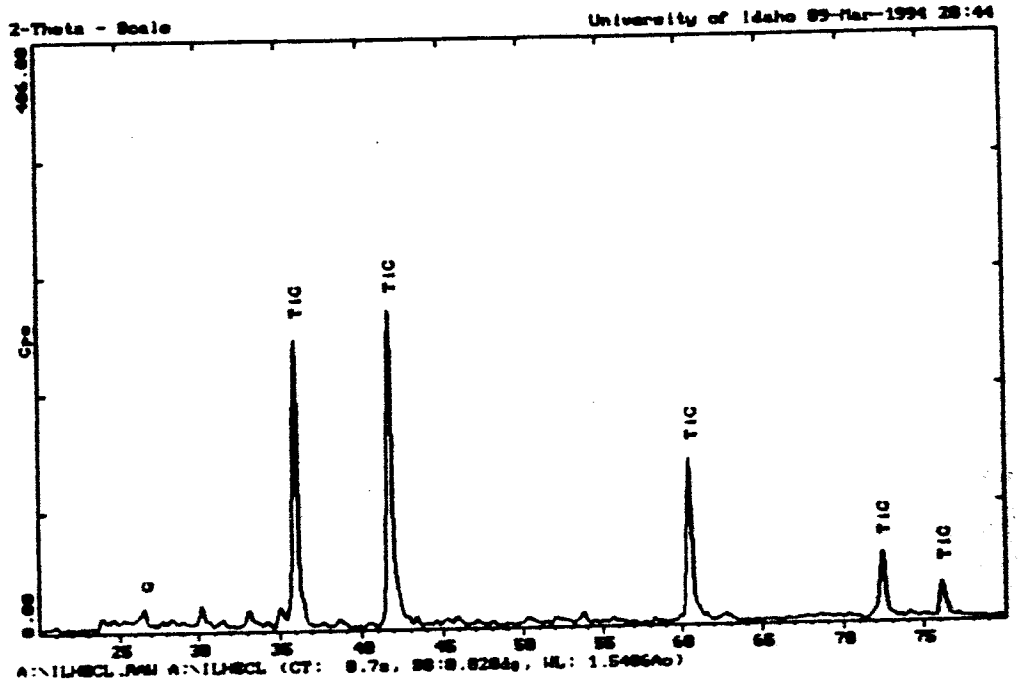

Fig. 7. X-ray diffraction patterns of the quench box solid product after leaching in HCl solution.

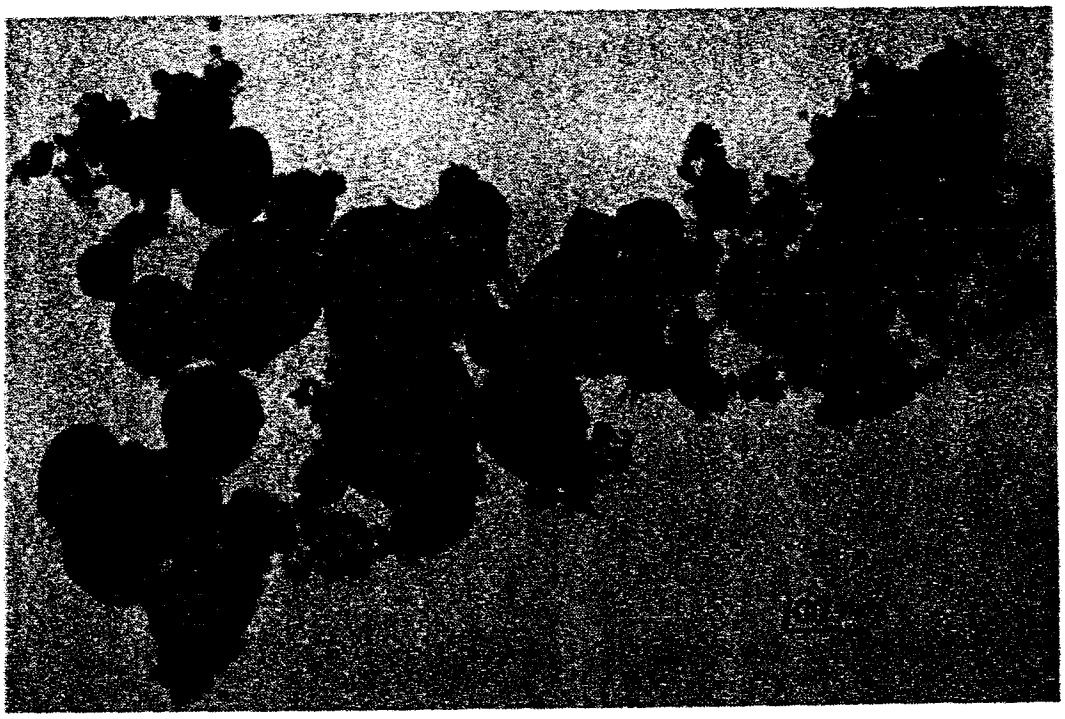

Fig. 8. TEM micrograph of the solid product collected from the quench box.

box product (after leaching with hydrochloric acid) from exp. TiC-4. It consisted mainly of TiC with a minor amount of graphite.

Samples from the different products were analyzed using SEM and microprobe techniques. Figure 8 shows a TEM micrograph of the powder collected from the quenching box (TiC-4). The powder size is mainly in the submicron range. A SEM micrograph of the quench box powder after HCl leaching is shown in Fig. 9a. This micrograph shows several types of particles with different shapes and sizes. These particles are shown at higher magnification in Fig. 9b, c, d and were identified by microprobe as zirconium carbide, silicon carbide, and titanium carbide, respectively.

6. CONCLUSIONS

Titanium carbide powder was produced directly from an ilmenite concentrate in a thermal plasma reactor.

Titanium/iron segregation during the plasma processing was observed, and may be a promising way to upgrade the ceramic product obtained from ilmenite concentrates.

Silicon carbide and zirconium carbide were identified as products obtained from the silica and zircon present as impurities in the ilmenite concentrates. These products may play an important role in the quality of the ceramic materials obtained by plasma processing of the ilmenite concentrates.

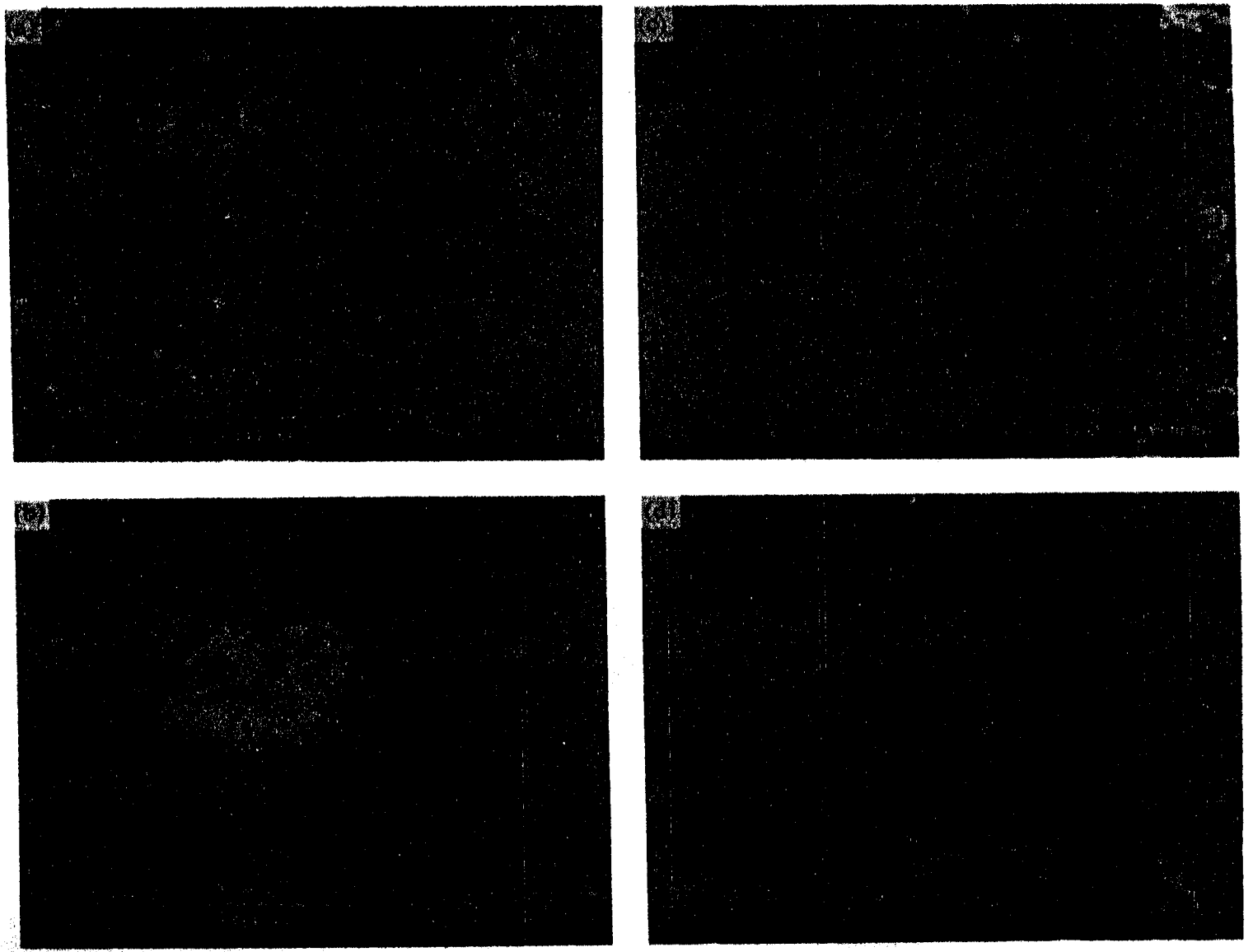

Fig. 9. (a) SEM micrograph of the quench box solid product after leaching in HCl solution; (b) a zirconium carbide particle; (c) a silicon carbide particle; (d) a titanium carbide particle; from the quench box solid product, identified by microprobe analysis.

Hydrochloric acid leaching may be feasible to remove iron from the plasma processing products, to obtain a final ceramic material useful in the industry.

ACKNOWLEDGMENT

The authors acknowledge the support of the National Science Foundation under grant No. CTS-9220252. One of the authors (Milton Manrique) acknowledges the support of CONICIT (Venezuela).

REFERENCES

1. T. P. Battle *et al.*, Proceedings of the Paul Queneau International Symposium on Extractive Metallurgy of Copper, Nickel, and Cobalt, Vol. 1, R. G. Reddy and R. N. Weizenbach, eds. TMS, Warrendale, Pennsylvania (1993), pp. 925–943.
2. S. Rao, *Miner. Met. Rev.*, **16**(7), 19–20 (1990).
3. J. L. Henry *et al.*, *U.S. Bur. Mines Bull.* **690** (1987).
4. G. W. Elger, *et al.*, *U.S. Bur. Mines Rep. Invest.* 9002, p. 24 (1985).
5. A. E. Raddatz *et al.*, *U.S. Bur. Mines Rep. Invest.* 8347, p. 10 (1978).
6. A. E. Back *et al.*, *U.S. Bur. Mines Rep. Invest.* 4902, p. 15 (1952).
7. J. M. Gomez, Proceedings 105th AIME Annual Meeting, S. R. Leavitt, ed., Las Vegas, Nevada, 1976, pp. 557–558.
8. D. A. Hansen and D. E. Traut, *J. Met.*, 34–36 (1989).
9. J. J. Leddy and D. L. Schechter, U. S. Patent 3, 060, 002 (1962).
10. Oster Felix, U.S. Patent 3, 787, 139 (1974).
11. R. D. Pike, U. S. Patent 2, 903, 341 (1959).
12. I. B. Ketteridge and R. E. Wilmshurst, *Aust. J. Appl. Sci.* **15**, 90–105 (1964).
13. C. Sankaran *et al.*, C. M. M. Extractive Metallurgy, pp. 480–500 (1967).
14. Y. Zhao and F. Shadman, *Ind. Eng. Chem. Res.* **30**, 2080–2087 (1991).
15. L. A. Taylor *et al.*, *Miner. Metall. Process.*, pp. 43–51 (1993).
16. K. S. Coley, B. S. Terry, and P. Grieveson, Proceedings T. Rosenqvist Symposium, S. E. Olsen and J. Kr. Tuset, eds., Trondheim, Norway (1988).
17. B. S. Terry and O. Chinyamakobvu, *Mater. Sci. Technol.* **7**, 842–848 (1991).
18. R. A. S. Brown, *Can. Metall. Q.* **10**, 47–55 (1971).
19. L. Yaozhong and Z. Z. Liu, Ph.D. Thesis, Kunming Institute of Technology, China (1989).
20. A. G. Turnbull and M. W. Wadsley, The CSIRO Thermochemistry System, Version 5, IMEC, Australia (1988).
21. P. R. Taylor, S. A. Pirzada, and T. D. McColm, Plasma Synthesis and Processing of Materials, K. Upadhya, ed., TMS, Warrendale, Pennsylvania (1993), pp. 179–190.